PHYSICAL REVIEW E, VOLUME 64, 011701

Thermal diffuse x-ray scattering in a model columnar liquid crystal

A. Lacombe and A. Caillé
Département de Physique, Université de Montréal, Casier Postal 6128, Succursale Centre-Ville, Montréal, Québec, Canada H3C 3J7

(Received 3 January 2001; published 11 June 2001)

The fluctuation correlation functions and the density-density correlation functions for a realistic model of a columnar liquid crystal in its helically ordered phase are derived. The influence of positional and orientational molecular fluctuations on the thermal diffuse x-ray scattering is studied within a three-dimensional model of columns inscribed on a triangular lattice. Resulting from quasi-long-range ordering, very anisotropic long-tail scattered intensities are predicted, giving a nonuniversal signature for the helically ordered columnar liquid crystal phase. Scattered intensities both near the Bragg maxima at the inverse lattice vectors and at the Bragg condition due to periodic orientational ordering are treated. The percolation of the long-range behavior for a screw variable composed of two quantities having only quasi-long-range behavior is predicted.

DOI: 10.1103/PhysRevE.64.011701 PACS number(s): 61.30.Cz, 61.30.Gd, 64.60.Cn, 64.70.Rh

I. INTRODUCTION

Molecular systems in their condensed state show a great diversity of ordered phases involving their positional and orientational degrees of freedom. Partial positional and orientational orderings are present in mesomorphous systems such as the liquid crystals. Unique and new fundamental structural properties emerge from the complexity and richness of such ordered phases. One such manifestation is the existence of quasi-long-range positional order in the layer ordering of smectic liquid crystals as revealed by high-resolution thermal diffuse x-ray scattering measurements [1–3].

Among such molecular systems, a number of compounds composed of disk-shaped molecules show columnar liquid crystal phases, all sharing a two-dimensional lattice ordering of columns of stacked molecules in the third direction. The types of positional and orientational ordering existing, in these cases, along the columns and their intercolumnar correlations are issues of a fundamental nature. One-dimensional liquidlike columns are usually observed, as predicted [4] by the divergent behavior of the local fluctuations of the intracolumnar positional degrees of freedom for a two-dimensional lattice of freely sliding columns in the third direction. However, there do exist materials [5–7] where a full or partial ordering of these degrees of freedom sets in at lower temperatures with a simultaneous ordering of the orientational degrees of freedom along the columns.

These last cases reveal a fundamental issue of classification: do they belong to the crystal phases or the mesomorphous phases? Up to now, this is still an open question [4,8–10]. However, the generally accepted understanding [5,6] calls for a long-range positional ordering inside the columns accompanied by an incommensurate helical orientational ordering of the diskotic molecules along the columns. This model, which is derived from the observed Bragg peak positions and intensities [5,6], is at least inconsistent with the very large value (at least one-third of the intermolecular spacing) of the phase-preserving vertical motion of the molecules [11] as measured from the Debye-Waller factors. Following these observations, in a previous publication [11], one of the authors has advanced the conjecture of quasi-long-range ordering of the positional and orientational degrees of freedom in such columnar liquid crystals. The vanishing of an effective shear elastic constant for strain deformations accompanied by a deformation of the orientational degrees of freedom would be at the origin of this behavior in such a soft material having a helically ordered state along the columns. As predicted [1] and observed [2,3] for smectic liquid crystals, thermal diffuse x-ray scattering in the presence of quasi-long-range ordering turns the Bragg peaks into Bragg maxima with a nonuniversal long-tail decrease of the scattered intensity in reciprocal space. Such behavior was conjectured in [11] for a particular columnar liquid crystal by involving only the thermal fluctuations of the positional degrees of freedom along the columns.

In this paper, using a simplified but realistic model that captures the essential features of these systems, we calculate the effects of the thermal fluctuations of both the positional and orientational degrees of freedom along the columns on the thermal diffuse x-ray scattering. Our objective is to make specific predictions on the power law behavior for the scattered intensity near the Bragg conditions resulting from both the ordering of the density of the molecules in the columnar direction and the incommensurate helical structure of their orientations. The three-column superlattice [5] existing for this frustrated intercolumnar structure is explicitly taken in account.

In Sec. II, the model is presented explicitly with a description of the core density modulation in three dimensions. To this core density is added an orientational feature that captures the gross features of the incommensurate helical structure. Section III presents the local root mean square (rms) fluctuations of the positional and orientational degrees of freedom as a function of the size of the sample in a direction perpendicular to the direction of columns which are otherwise of infinite length. In Sec. IV, the correlation functions for the density and orientational features are reported with their specific behavior in two directions, namely, parallel and perpendicular to the columns. Section V presents the calculations of thermal diffuse x-ray scattering intensities and their shapes in reciprocal space near the Bragg maxima. The calculations put the emphasis on the long-tail behavior of the intensity of the scattered x rays for fluctuations controlled by

1063-651X/2001/64(1)/011701(16)/$20.00

quasi-long-range ordering. The classical behavior, with a q^{-2} decrease, for fluctuating variables controlled by long-range ordering is assumed to exist and to be buried under the nonclassical behavior due to quasi-long-range behavior. Finally, the last section refers to specific interpretations and conclusions leading to further measurements of high-intensity and high-resolution diffuse x-ray scattering from these systems.

II. MODEL PRESENTATION

The molecular model for a liquid crystal made of disk-shaped molecules stacked into columns regularly placed onto a two-dimensional lattice, a structure known as a diskotic, has already been investigated in detail [5]. An example of such a liquid crystal is given by hexa-hexylthiotriphenylene (HHTT), one of the triphenylene derivatives whose molecules are formed of a rigid core of aromatic cycles and six flexible hydrocarbon chains fixed to the core. This compound shows two distinct hexagonal columnar phases: D_{hd}, a disordered columnar phase ($70\,°\mathrm{C}<T<93\,°\mathrm{C}$), and H, a helically ordered columnar phase ($62\,°\mathrm{C}<T<70\,°\mathrm{C}$). This last phase is of great interest since it could reveal, under given conditions, quasi-long-range intracolumnar order as proposed in [11]. In the H phase, the lattice that supports the columns is reorganized in a superlattice $\sqrt{3}\times\sqrt{3}R30°$ which is spanned by the set of vectors

$$\vec{a}_1=\frac{a}{2}(3\hat{x}+\sqrt{3}\hat{y}), \tag{1a}$$

$$\vec{a}_2=a\sqrt{3}\hat{y}, \tag{1b}$$

$$\vec{c}_1=c\hat{z}, \tag{1c}$$

where a is the distance between the centers of the columns in the basal plane and c is the distance between the molecules in the columns if long-range ordering is assumed as illustrated in Figs. 1(a) and 1(b). The superlattice conventional cell basis has three HHTT molecules located respectively at $\vec{r}_j$ with $\vec{r}_0=\vec{0}$, $\vec{r}_1=\frac{1}{3}(\vec{a}_1+\vec{a}_2)+\frac{1}{2}\vec{c}_1$, and $\vec{r}_2=\frac{2}{3}(\vec{a}_1+\vec{a}_2)+\frac{1}{2}\vec{c}_1$ as shown in Fig. 1(a). The reciprocal lattice vectors associated with this lattice are given by $\vec{K}_i(\vec{n})=n_1\vec{A}_1+n_2\vec{A}_2+n_3\vec{C}_1$ where n_1,n_2, and n_3 are integers and

$$\vec{A}_1=\frac{4\pi}{3a}\hat{x}, \tag{2a}$$

$$\vec{A}_2=\frac{2\pi}{a}\left(\frac{1}{\sqrt{3}}\hat{y}-\frac{1}{3}\hat{x}\right), \tag{2b}$$

$$\vec{C}_1=\frac{2\pi}{c}\hat{z}. \tag{2c}$$

For quasi-long-range order, this superlattice would have a meaning in the $\hat{z}$ direction only over a finite but extremely long distance measured on a molecular scale.

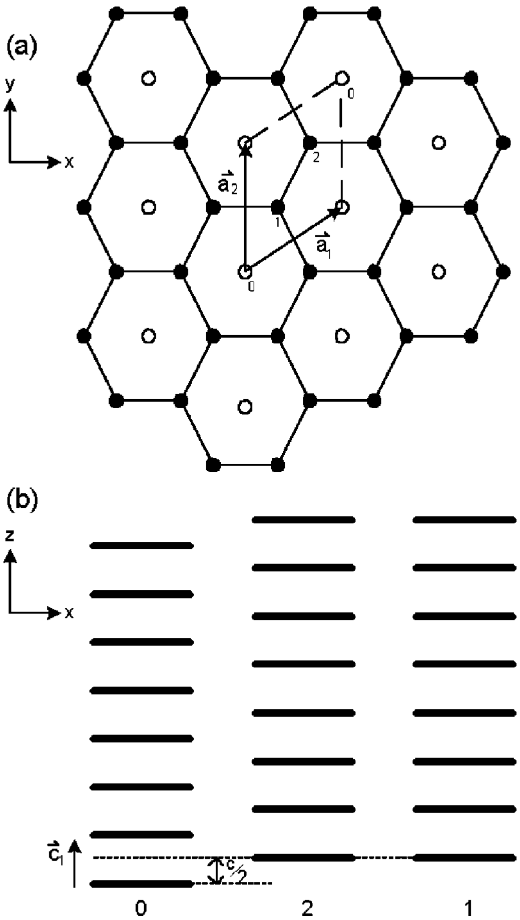

FIG. 1. (a) Top view of the two-dimensional columnar structure, the full black dots (labeled 1 and 2) being the displaced columns and the open dots (labeled 0) the undisplaced columns. (b) Three-dimensional side view of the molecular stacks in three different columns in their equilibrium configurations if long-range ordering is assumed.

We choose to represent the density of molecules in the three-dimensional system by a development in a Fourier series which captures the essential features of the overall density modulation and which is called here the *core density*. The lower-order components are sufficient for the study of the conversion of the lower-order Bragg peaks into Bragg maxima and the calculations of the thermal diffuse scattering near those Bragg peaks. The coefficients of the Fourier series are chosen such that the core density (i) is real and positive everywhere, (ii) exhibits invariance with respect to a rotation of $2n\pi/6$ around the center of the zeroth column of every cell, and (iii) is such that the maxima of the density for the columns numbered 1 and 2 are shifted by $c/2$ along the columnar axis with respect to the maxima of the columns numbered 0 [5]. Consequently, the equilibrium core density $\rho_{0c}(\vec{r})$, for an ordering extending to infinity, is written as

$$\rho_{0c}(\vec{r})=b_0+\sum_{i\neq 0} b_{\vec{K}_i}\cos(\vec{K}_i\cdot\vec{r}), \tag{3}$$

where the specific relations between the real coefficients $b_{\vec{K}_i}$ are given below in order to satisfy the criteria mentioned above. For the purpose of calculating the density-density correlation functions appearing in the expression of the thermal diffuse scattering intensities near the lower-order Bragg peaks, only a finite number of inverse lattice vectors have been selected, resulting in a spatial density continuum instead of a discrete matter distribution. These vectors $\vec{K}_i$ are

$$\vec{K}_i \in \{\vec{C}_1, \vec{A}_1+\vec{C}_1, \vec{A}_1-\vec{C}_1, \vec{A}_2+\vec{C}_1, \vec{A}_2-\vec{C}_1, -(\vec{A}_1+\vec{A}_2)+\vec{C}_1, -(\vec{A}_1+\vec{A}_2)-\vec{C}_1\} \cup \{2\vec{A}_1+\vec{A}_2, -\vec{A}_1+2\vec{A}_2, \vec{A}_2-\vec{A}_1\}. \tag{4}$$

The first subset contains seven vectors describing the superlattice density and hence gives no information about the inner-cell structure. Only the three vectors in the second subset of Eq. (4) generate an intracellular density modulation corresponding to the structure of the basis. The real coefficients $b_{\vec{K}_i}$ associated with the different $\vec{K}_i$'s must satisfy the following relations:

$$b_0 = \sum_{i=1}^{10} b_{\vec{K}_i}, \tag{5a}$$

$$b_{\vec{K}_2} = b_{\vec{K}_3} = b_{\vec{K}_4} = b_{\vec{K}_5} = b_{\vec{K}_6} = b_{\vec{K}_7}, \tag{5b}$$

$$b_{\vec{K}_8} = b_{\vec{K}_9} = b_{\vec{K}_{10}}, \tag{5c}$$

and

$$b_{\vec{K}_1} = -\frac{1}{4}\left(\sum_{i=2}^{7} b_{\vec{K}_i}\right), \tag{5d}$$

where the vectors $\vec{K}_i$ are numbered in the order they appear in Eq. (4): $\vec{K}_1 = \vec{C}_1$, $\vec{K}_2 = \vec{A}_1 + \vec{C}_1$, $\vec{K}_3 = \vec{A}_1 - \vec{C}_1$, and so on (note that $\vec{K}_0 = \vec{0}$). The condition (5a) ensures that ρ_{0c} is positive everywhere; (5b) and (5c) result from the rotational invariance constraint (ii) described above while (5d) follows from the constraint (iii). The equilibrium core density continuum is illustrated in Fig. 2. The superlattice structure in the basal plane is easily seen as well as the displacement in the columnar direction of two-thirds of the columns.

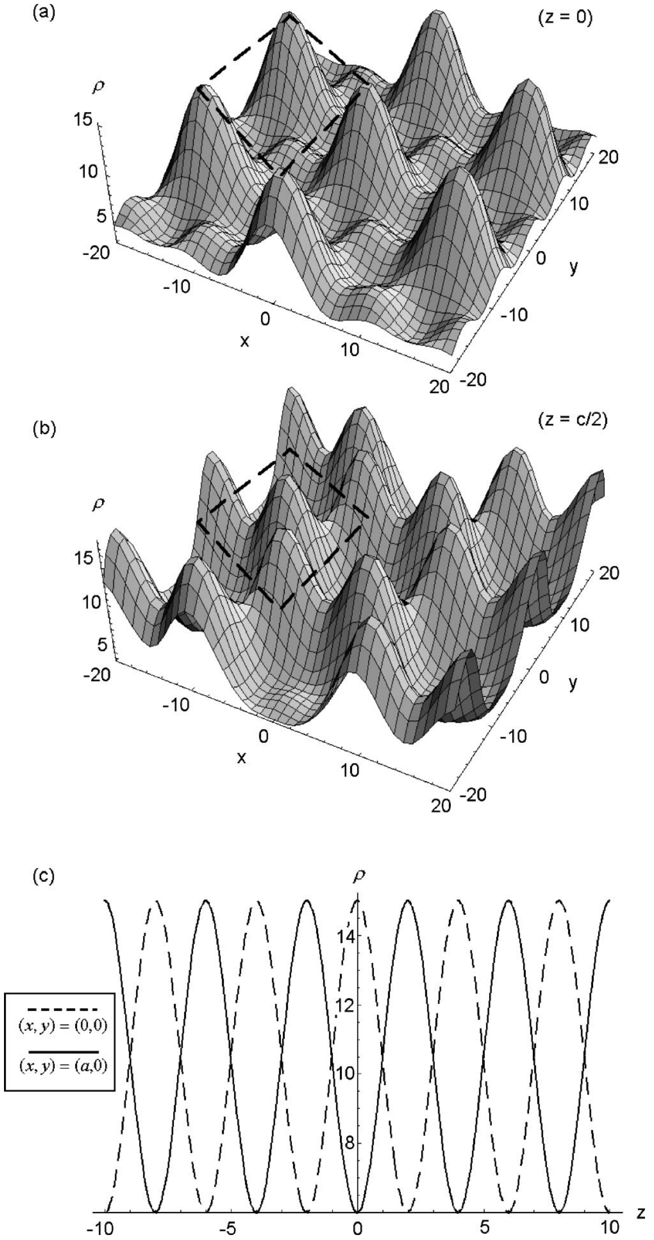

FIG. 2. The equilibrium core density continuum (a) at $z=0$ in the basal plane; (b) at $z=c/2$ in the basal plane; (c) at $(x,y)=(0,0)$ and $(x,y)=(a,0)$ as a function of z. In (a) and (b), the unit cell is represented schematically showing the presence of maxima at the corners of the cell in (a) and two maxima inside the cell in (b). Arbitrary values have been used ($a=10$, $c=4$, and the coefficients b_2 to b_{10} were all set to unity). x and y have the same units as a, z has the same units as c, and ρ has the same units as ρ_0 and b_{K_i}.

The second feature to capture in the density is the helical modulation appearing as we move along the columnar direction. For the purpose of representing this density modulation, a term is added to Eq. (3). This term accounts for the geometry and orientation of HHTT molecules. Effectively, these disklike molecules in their propeller configuration [6] show a rotational invariance of $2n\pi/3$ around an axis passing through their center, perpendicularly to their planar central core. Thus, around every site along the column j, a supplementary density modulation proportional to $\cos 3[\theta - \theta_{0j}(z)]$ is added on a circle of radius R_0 placed perpendicularly to the columnar direction and centered on the site as depicted in Fig. 3. R_0 is the mean radius of the molecular columns which are extending in the z direction. The phase $\theta_{0j}(z)$, representing the angular shift of the molecules along the column j in the equilibrium helical conformation, is written as

$$\theta_{0j}(z) = H_j \omega z + \Omega_j, \tag{6}$$

where H_j and Ω_j are, respectively, the helicity ($H_j = \pm 1$) and the rigid angular shift of the column j. ω equals $2\pi/P$ where P is the pitch of the column. In the present model, P will be taken close to $8c$, every molecule being rotated by an amount close to $\pi/4$ from its nearest neighboring molecule inside a given column. Incommensurability between the pitch and the lattice distance has been assumed for the

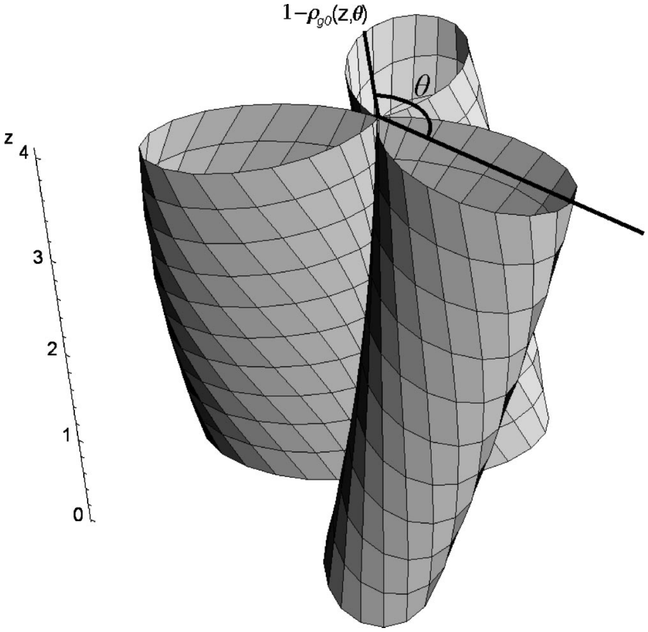

FIG. 3. Groove density modulation $[1-\rho_{g0}(z,\theta)]$ along a continuous column of stacked molecules. Arbitrary values have been used ($\rho_0=1, c=4, H_j=1$, and $\Omega_j=0$). z has the same units as c.

present work even though this is still an open question [13]. Also, the rotational invariance constraint (ii) implies that $H_1=H_2$ and $\Omega_1=\Omega_2$. In the present model, this helicoidal density engraving is called the *groove density* and is written as

$$\rho_{g0}(\vec{r})=\rho_0\sum_{n,m}\sum_{j=0}^{2}\delta(\vec{\rho}-(\vec{\rho}_{nm}+\vec{\rho}_j+\vec{\sigma}))\times\cos 3(\theta-H_j\omega z-\Omega_j), \tag{7}$$

where cylindrical coordinates have been used. $\vec{r}=(\vec{\rho},z)$ with $\vec{\rho}=(\rho,\alpha_\perp)$, as illustrated in Fig. 4. The discrete molecular density modulation has been represented, for simplicity, by a continuous cylindrical surface density modulation. These density modulation cylinders of radius R_0 are centered on the lattice points given by $\vec{\rho}_{nm}+\vec{\rho}_j$ where $\vec{\rho}_{nm}=n\vec{a}_1+m\vec{a}_2$ and $\vec{\rho}_j=\frac{j}{3}(\vec{a}_1+\vec{a}_2)$ with $j\in\{0,1,2\}$. Finally, $\vec{\sigma}$ $[\vec{\sigma}=(R_0,\theta)]$ points at a specific location on the surface density modulation cylinder (see Fig. 4). The constant coefficient ρ_0 in Eq. (7) is chosen to ensure that the total density remains positive everywhere. Thus, the total equilibrium density, according to the model developed here for the HHTT diskotic liquid crystal in its H phase, is given by $\rho_0(\vec{r})=\rho_{c0}(\vec{r})+\rho_{g0}(\vec{r})$. Although this separation of the density modulation into two terms is not derived from first principles, it has the advantage of capturing the essential features affecting the diffuse x-ray scattering near the lower-order Bragg peaks.

III. LOCAL CORRELATION FUNCTIONS

In this section, the local root mean square fluctuations of the positional and orientational degrees of freedom of the molecules are presented. In the next section, these results are used to establish the behavior of the density-density correlation function $\langle\rho(\vec{r})\rho(\vec{r}\,')\rangle$ along specific directions in our columnar liquid crystal model. The details of the calculations are presented in the Appendix.

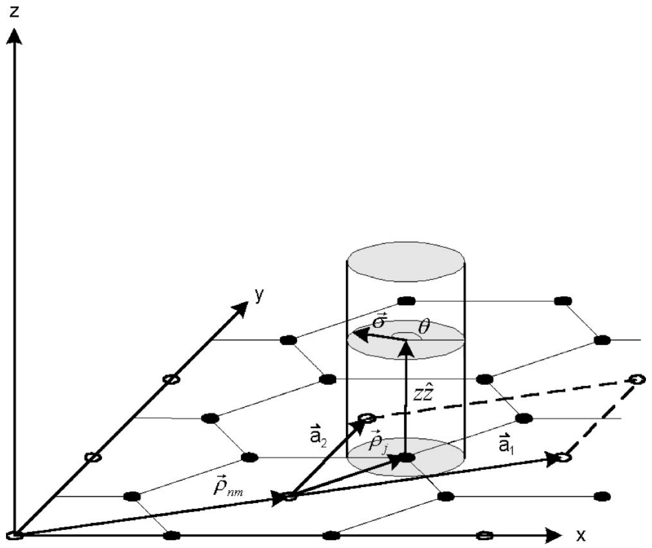

FIG. 4. Representation of the vectors $\vec{r}$, $\vec{\rho}$, and $\vec{\sigma}$ used to locate a point on the surface of molecular cylinders.

Among all the possible positional fluctuations of the molecules, only the displacement $u_z(\vec{r})$ along the columnar direction has been considered. This limitation will be justified later in Sec. VI. The orientational fluctuations of the molecules are described by $\varphi(\vec{r})$, an angular variable specifying a rotation in the plane perpendicular to the columns with respect to the helical equilibrium conformation. The planar positional fluctuations $u_{q_\perp}(\vec{r})$ have not been considered in the density fluctuations since they are known to have long-range behavior in this phase [4]. The fluctuating density is written as $\rho(\vec{r})=\rho_0[\vec{r}-u_z(\vec{r})\hat{z}]$ where ρ_0 represents the density of the system at $T=0$ K [12]. Taking $\rho_{c0}(\vec{r})+\rho_{g0}(\vec{r})$ as the equilibrium density ρ_0, the fluctuations are introduced in both $\rho_{c0}(\vec{r})$ and $\rho_{g0}(\vec{r})$ according to

$$\rho_c(\vec{r})=b_0+\sum_{i\neq 0}b_{\vec{K}_i}\cos\{K_{i\perp}\rho\cos(\alpha_\perp-\alpha_i)+K_{iz}(z-u_z[\vec{r}])\} \tag{8}$$

for the fluctuating core density and to

$$\rho_g(\vec{r})=\rho_{g0}\sum_{n,m}\sum_{j=0}^{2}\delta(\vec{\rho}-(\vec{\rho}_{nm}+\vec{\rho}_j+\vec{\sigma}))\times\cos 3\{\theta-H_j\omega[z-u_z(\vec{r})]-[\Omega_j-\varphi(\vec{r})]\} \tag{9}$$

for the fluctuating groove density. α_i is the angle between $\vec{K}_i$ and $\hat{x}$.

A derivation of the total elastic energy, based on the orientational and positional elastic energy densities, was carried out by one of the authors in [11]. The diagonalized form of this total elastic energy, expressed in Fourier space using cylindrical coordinates, is given by

$$E=\frac{1}{2}\frac{1}{(2\pi)^3}\int d^3q\left\{\left[g_1-\frac{\gamma^2}{4g_2}\right]|u_z(\vec{q})|^2+g_2|u'_{q_\perp}(\vec{q})|^2+\left[\frac{1}{4}C_5q_z^2+C_3q_\perp^2\right]|u_\theta(\vec{q})|^2+f|\Psi(\vec{q})|^2\right\} \tag{10}$$

where the functions $g_1(\vec{q})$, $g_2(\vec{q})$, $\gamma(\vec{q})$, $f(\vec{q})$, $a(\vec{q})$, and $b(\vec{q})$ are defined in [11]. The quantities A_i, B_i, C_i, and K_i appearing here or in the following equations are the elastic constants introduced in [11]. In the process of diagonalization, two successive changes of variables are introduced, leading to

$$\varphi(\vec{q})=\Psi(\vec{q})-\frac{b}{2f}u_z(\vec{q})-\frac{a}{2f}u_{q_\perp}(\vec{q}) \tag{11}$$

and

$$u_{q_\perp}(\vec{q})=u'_{q_\perp}(\vec{q})-\frac{\gamma}{2g_2}u_z(\vec{q}). \tag{12}$$

From Eq. (10), the theorem of equipartition yields

$$\langle|u_z(\vec{q})|^2\rangle_T=\frac{k_BT}{g_1-\dfrac{\gamma^2}{4g_2}}, \tag{13a}$$

$$\langle|u'_{q_\perp}(\vec{q})|^2\rangle_T=\frac{k_BT}{g_2}, \tag{13b}$$

$$\langle|u_\theta(\vec{q})|^2\rangle_T=\frac{k_BT}{\dfrac{1}{4}C_5q_z^2+C_3q_\perp^2}, \tag{13c}$$

and

$$\langle|\Psi(\vec{q})|^2\rangle_T=\frac{k_BT}{f} \tag{13d}$$

for the rms fluctuations expressed in Fourier space. The angular brackets with the subscript T denote an average over all the thermal states.

In the long-wavelength limit, the denominator of Eq. (13a) has the following power expansion for $q_\perp \ll q_z$:

$$g_1-\frac{\gamma^2}{4g_2}=C_1q_z^2+Gq_\perp^2, \tag{14}$$

where $G=C_5/4-(C_4+\frac{1}{2}C_5)^2/2C_5$. Equation (14) is typical of a denominator for long-range ordering where the local rms fluctuation of the vertical displacement would have a microscopic value proportional to a molecular length, a value independent of the size of the system.

For $q_z \ll q_\perp$, the long-wavelength limit expression for the denominator becomes

$$g_1-\frac{\gamma^2}{4g_2}=C_1q_z^2+Kq_\perp^4, \tag{15}$$

where $K=B_2^2(K_1+K2)/8A_1^2$, provided that the hypothesis of an effective free sliding of ordered columns on each other is realized [11].

The thermal and space average $\langle u_z^2(\vec{r})\rangle$ is given by

$$\langle u_z^2(\vec{r})\rangle=\frac{1}{V}\frac{1}{(2\pi)^3}\int d^3q\langle|u_z(\vec{q})|^2\rangle_T, \tag{16}$$

where V is the volume of the system. The integral in Eq. (16) is dominated by a size dependent term arising from the integrand in the long-wavelength limit and $q_z \ll q_\perp$. The rest of the integral adds only size independent terms of microscopic magnitude. The size dependent term is easily shown to be given by

$$\langle u_z^2(\vec{r})\rangle=\frac{k_BT}{4\pi\sqrt{KC_1}}\ln\left(\frac{L_\perp}{a}\right), \tag{17}$$

an expression involving only the size $L_\perp$ of the system in a direction perpendicular to the columns with otherwise infinite length. This expression, which increases progressively but slowly with the length $L_\perp$, is typical of quasi-long-range order [11].

The calculation of $\langle u_z(\vec{r})\varphi(\vec{r})\rangle$ is carried out in Sec 1 of the Appendix using the residue theorem in the complex plane and yields

$$\langle u_z(\vec{r})\varphi(\vec{r})\rangle=\frac{-k_BT}{4\pi\sqrt{KC_1}}\frac{B_2}{8A_1}\ln\left(\frac{L_\perp}{a}\right) \tag{18}$$

under the same approximations as above. Again, this result involves only the size of the sample in the direction perpendicular to the columns.

The third local rms fluctuation correlation function $\langle\varphi^2(\vec{r})\rangle$, involves three separate integrations over the Fourier space since the diagonalized form of $\varphi(\vec{r})$ is the sum of three independent fluctuating quantities according to Eqs. (11) and (12). The final result is given by

$$\langle\varphi^2(\vec{r})\rangle=\frac{k_BT}{4\pi\sqrt{(K_1+K_2)A_2}}\ln(K'+\sqrt{K'^2+1})+\frac{k_BT}{4\pi\sqrt{KC_1}}\frac{B_2^2}{16A_1^2}\ln\left(\frac{L_\perp}{a}\right)+C'\frac{k_BT}{a}\frac{(B_1+B_2)^2}{A_2^2C_5}, \tag{19}$$

where K' and C' are constants defined in Sec. 1 of the Appendix. A striking feature of the first and third terms of Eq. (19) is that they are independent of the size of the sample. These terms arise, respectively, from the integration of $\langle|\Psi(\vec{q})|^2\rangle_T$ and $(a^2/4f^2)\langle|u'_{q_\perp}(\vec{q})|^2\rangle_T$ over the Fourier space, indicating that these quantities have behaviors typical of long-range ordering.

IV. FLUCTUATION CORRELATION FUNCTIONS AND DENSITY-DENSITY CORRELATION FUNCTIONS

The density-density correlation functions involve not only the local fluctuation correlation functions but also the fluctuation correlation functions. $\langle u_z(\vec{r})u_z(\vec{r}\,')\rangle$, $\langle u_z(\vec{r})\varphi(\vec{r}\,')\rangle$, $\langle u_z(\vec{r}\,')\varphi(\vec{r})\rangle$, and $\langle \varphi(\vec{r})\varphi(\vec{r}\,')\rangle$ are obtained in the next subsection. The density-density correlation functions are then calculated using these results and those of Sec. III.

A. Fluctuation correlation functions in the columnar direction

In this subsection, only the results are presented, the reader being referred to Sec. 2 of the Appendix for further mathematical details. The first correlation function of interest is $\langle u_z(\vec{r})u_z(\vec{r}\,')\rangle$. Assuming overall translational invariance, it is given by

$$\langle u_z(\vec{r})u_z(\vec{r}\,')\rangle=\int \frac{d^3q}{(2\pi)^3}\langle|u_z(\vec{q})|^2\rangle_T e^{-i\vec{q}\cdot(\vec{r}-\vec{r}\,')}. \quad (20)$$

Let us start with the correlation for large separation along the columns, i.e., $|z-z'|\gg c$ and $|\rho-\rho'|$ of the order of a. As a result, the integral (20) is dominated by the small q_z contributions where $q_\perp$ extends from its lower limit $2\pi/L_\perp$ to $2\pi/a$. Consequently, $\langle|u_z(\vec{q})|^2\rangle$ is governed by the denominator (15). As shown in the Appendix, $\langle u_z(\vec{r})u_z(\vec{r}\,')\rangle$ is then given by

$$\langle u_z(\vec{r})u_z(\vec{r}\,')\rangle=\frac{-k_BT}{8\pi\sqrt{KC_1}}\left[2\gamma+E_1\left(\frac{(\rho-\rho')^2}{4\beta|z-z'|}\right)+\ln\left(\frac{\pi^2(\rho-\rho')^2}{L_\perp^2}\right)\right]. \quad (21)$$

It has been assumed in the calculation of Eq. (21) that $\vec{\rho}$ is parallel to $\vec{\rho}\,'$ since only quantities dependent on $\vec{\rho}-\vec{\rho}\,'$ will be needed in the subsequent calculations. The fluctuation correlation function $\langle u_z(\vec{r})\varphi(\vec{r}\,')\rangle$, under similar conditions, is given by

$$\langle u_z(\vec{r})\varphi(\vec{r}\,')\rangle=\frac{k_BT}{8\pi\sqrt{KC_1}}\frac{B_2}{4A_1}\left[2\gamma+E_1\left(\frac{(\rho-\rho')^2}{4\beta|z-z'|}\right)+\ln\left(\frac{\pi^2(\rho-\rho')^2}{L_\perp^2}\right)\right]. \quad (22)$$

The fluctuation correlation function $\langle\varphi(\vec{r})\varphi(\vec{r}\,')\rangle$ involves three separate integrations, as in Eq. (A9). Assuming again that $\vec{\rho}$ is parallel to $\vec{\rho}\,'$, this quantity, under the same conditions as above, is given by

$$\langle\varphi(\vec{r})\varphi(\vec{r}\,')\rangle=\frac{k_BT}{8\pi}\sum_{i=1}^{4}\frac{\xi_i}{\sqrt{\kappa_i(z-z')^2+(\rho-\rho')^2}}-\frac{k_BT}{8\pi\sqrt{KC_1}}\frac{B_2^2}{16A_1^2}\left[2\gamma+E_1\left(\frac{(\rho-\rho')^2}{4\beta|z-z'|}\right)+\ln\left(\frac{\pi^2(\rho-\rho')^2}{L_\perp^2}\right)\right], \quad (23)$$

where the constant coefficients ξ_i and κ_i are defined in the Appendix.

B. Fluctuation correlation functions in the direction perpendicular to the columns

As shown in Sec. 3 of the Appendix, the fluctuation correlation functions at large separation in the plane perpendicular to the columns for a separation along the columns of a molecular size ($|z-z'|\sim c$ and $|\rho-\rho'|\gg a$) follow a behavior typical of long-range ordering. Effectively, under these conditions, the integral (20) is dominated by the small $q_\perp$ contributions where q_z extends from $-\infty$ to ∞, the denominator in action being given by Eq. (14).

C. Density-density correlation functions in the columnar direction

In this subsection, the behavior of the density-density correlation function $G(\vec{r}-\vec{r}\,')=\langle\rho(\vec{r})\rho(\vec{r}\,')\rangle$ is presented for the columnar direction. According to the present model, this function is given by

$$\begin{aligned}G(\vec{r}-\vec{r}\,')&=\langle\rho(\vec{r})\rho(\vec{r}\,')\rangle\\&=\langle[\rho_c(\vec{r})+\rho_g(\vec{r})][\rho_c(\vec{r}\,')+\rho_g(\vec{r}\,')]\rangle\\&=\langle\rho_c(\vec{r})\rho_c(\vec{r}\,')\rangle+\langle\rho_c(\vec{r})\rho_g(\vec{r}\,')\rangle\\&\quad+\langle\rho_g(\vec{r})\rho_c(\vec{r}\,')\rangle+\langle\rho_g(\vec{r})\rho_g(\vec{r}\,')\rangle,\end{aligned} \quad (24)$$

where the angular brackets denote spatial and thermal averages, and $\rho(\vec{r})$ and $\rho(\vec{r}\,')$ are given by Eqs. (8) and (9). These calculations are performed by using the fact that for fluctuating quantities x_i subject to a Gaussian distribution the relation

$$\langle\exp[\alpha_i x_i]\rangle_T=\exp[\alpha_i\alpha_k\langle x_i x_k\rangle_T/2], \quad (25)$$

where the α_i are constants, always holds [12]. It is found, as detailed in Sec. 4 of the Appendix, that only the terms $\langle\rho_c(\vec{r})\rho_c(\vec{r}\,')\rangle$ and $\langle\rho_g(\vec{r})\rho_g(\vec{r}\,')\rangle$ contribute to $G(\vec{r}-\vec{r}\,')$. Effectively, the mixed terms $\langle\rho_c(\vec{r})\rho_g(\vec{r}\,')\rangle$ and $\langle\rho_g(\vec{r})\rho_c(\vec{r}\,')\rangle$ vanish in the averaging process over thermal states unless $K_{iz}=\pm3(H_j\omega\pm B_2/4A_1)$, or $K_{iz}=\pm3(H_{j'}\omega\pm B_2/4A_1)$, conditions that are too restrictive.

The behavior of the first term of $G(\vec{r}-\vec{r}\,')$ along the columnar direction (for $|z-z'|\gg c$ and $|\rho-\rho'|\simeq a$) is given by

$$\langle\rho_c(\vec{r})\rho_c(\vec{r}\,')\rangle\sim\sum_i b_{\vec{K}_i}^2\cos\vec{K}_i\cdot(\vec{r}-\vec{r}\,')\times\left(\frac{a^2}{4\pi^2\beta|z-z'|}\right)^{X(K_{iz})}, \tag{26}$$

with

$$X(K_{iz})=K_{iz}^2\frac{k_bT}{8\pi\sqrt{KC_1}}. \tag{27}$$

The behavior of the last term is given by

$$\langle\rho_g(\vec{r})\rho_g(\vec{r}\,')\rangle\sim\sum_{n,m}\sum_{n',m'}\sum_{j=0}^{2}\sum_{j'=0}^{2}F_2\left(\frac{a^2}{4\pi^2\beta|z-z'|}\right)^{X'_j} \tag{28}$$

within the same limit as in Eq. (26), with

$$F_2=\delta(\vec{\rho}-(\vec{\rho}_{nm}+\vec{\rho}_j+\vec{\sigma}))\delta(\vec{\rho}\,'-(\vec{\rho}_{n'm'}+\vec{\rho}_{j'}+\vec{\sigma}\,'))\times\cos 3[\theta-H_j\omega z-\Omega_j-(\theta'-H_{j'}\omega z'-\Omega_{j'})] \tag{29}$$

and

$$X'_j=\frac{9k_bT}{8\pi\sqrt{KC_1}}\left(\frac{B_2}{4A_1}-H_j\omega\right)^2. \tag{30}$$

This last exponent involves explicitly the value of the helicity of the jth column.

D. Density-density correlation function in a direction perpendicular to the columns

In parallel with the results reported in Sec. IV B, the density-density correlation functions at large separation in the plane perpendicular to the columns ($|z-z'|\sim c$ and $|\rho-\rho'|\gg a$) are, under the above conditions, typical of long-range ordering. As a result, they are periodic functions with the periods of the columns in the two-dimensional basal plane.

V. X-RAY SCATTERED INTENSITIES

In this section, the scattered intensities for both the nonfluctuating and the fluctuating equilibrium conformations of our model are presented. The general expressions found for the density-density correlation functions derived above are used.

A. The Bragg conditions of the model

The x-ray scattering intensity for a momentum transfer $\vec{Q}$ is obtained directly from the Fourier transforms of $\rho_c(\vec{r})$ according to

$$I(\vec{Q})\propto\int d^3r\int d^3r'\,\rho(\vec{r})\rho(\vec{r}\,')e^{i\vec{Q}\cdot(\vec{r}-\vec{r}\,')}, \tag{31}$$

where proportionality constants are omitted. The scattering intensity is decomposed into three terms according to

$$I(\vec{Q})=I_{cc}(\vec{Q})+I_{cg}(\vec{Q})+I_{gg}(\vec{Q}). \tag{32}$$

The indices refer to the different combinations of core density and groove density in the decomposition of the total density $\rho(\vec{r})$. It is easily shown that the mixed term I_{cg} does not contribute and that I_{cc} is the only term contributing to the scattering near the inverse lattice vectors, and conversely only the term I_{gg} contributes for scattering near the Bragg condition due to the periodic orientational density. In the absence of thermal fluctuations, the result is

$$I(\vec{Q})\propto\sum_i b_{\vec{K}_i}^2\delta_{\vec{Q},\pm\vec{K}_i}+\rho_{g0}^2J_3^2(Q_\perp R_0)\times\left[1+4\sin^2\left(\frac{2}{3}\vec{Q}_\perp\cdot(\vec{a}_1+\vec{a}_2)\right)\right]\delta_{Q_z,\pm 3\omega}\delta_{\vec{Q}_\perp,\vec{K}_{hk}}, \tag{33}$$

where $\vec{K}_{hk}=p\vec{A}_1+k\vec{A}_2$ and J_3 is the third order Bessel function. The first term in Eq. (33) is proportional to the Fourier transform of $\rho_c(\vec{r})\rho_c(\vec{r}\,')$, while the second term is proportional to the Fourier transform of $\rho_g(\vec{r})\rho_g(\vec{r}\,')$. The scalar product in this latter term could be rewritten as

$$\frac{2}{3}\vec{Q}_\perp\cdot(\vec{a}_1+\vec{a}_2)=\frac{4\pi}{3}(p+k) \tag{34}$$

since $\vec{Q}_\perp=p\vec{A}_1+k\vec{A}_2$.

B. The thermal diffuse x-ray scattering near the reciprocal lattice vectors

The scattered intensity of x rays for a momentum transfer $\vec{Q}$ when the thermal fluctuations are included is given by

$$I(\vec{Q})=\int d^3r\int d^3r'\langle\rho(\vec{r})\rho(\vec{r}\,')\rangle e^{i\vec{Q}\cdot(\vec{r}-\vec{r}\,')}, \tag{35}$$

where $\langle\rho(\vec{r})\rho(\vec{r}\,')\rangle$ is the density-density correlation function averaged over the thermal fluctuations. We now consider a momentum transfer $\vec{Q}$ close to the reciprocal lattice vectors $\vec{K}_i$ such that $\vec{Q}=\vec{K}_i+\vec{q}_\perp+q_z\hat{z}$ where $\vec{q}_\perp$ and q_z are very small on the scale of the inverse of their respective intermolecular distances.

Within our model, the scattering intensity near the reciprocal lattice vectors is limited to the basal plane $K_{iz}=0$ and the planes $\vec{K}_{iz}=\pm\vec{C}_1$. The shapes of the Bragg peaks in the basal plane $K_{iz}=0$ are easily predicted. Indeed, only the thermal fluctuations of the perpendicular component $\vec{u}_\perp$ determine the diffuse scattering of the x rays for a zero value of K_{iz}. Since this quantity reflects the long-range ordering in the basal plane, the Bragg peaks in this plane maintain their character with an intensity controlled by a Debye-Waller factor and a decrease in reciprocal space that is inversely proportional to the square of the wave-number departure from the Bragg positions.

For the planes at $\vec{K}_{iz}=\pm\vec{C}_1$, the thermal fluctuations of u_z turn the Bragg peaks into Bragg maxima with a nonuniversal behavior of the power law decrease of the scattered intensity in reciprocal space. Near the Bragg conditions for the lattice, the scattered intensity is written as

$$I_{cc}(q_z,\vec{q}_\perp)\propto\int d^3r e^{iq_z z}e^{i\vec{q}_\perp\cdot\vec{\rho}}[e^{i\vec{K}_i\cdot\vec{r}}\langle\rho_c(\vec{r})\rho_c(0)\rangle]. \tag{36}$$

For $q_z\simeq 0$ and $q_\perp \gg q_z$, the integral (36) is dominated by a cone surrounding the z axis and extending to infinity. The correlation function of the fluctuating displacements in this cone is then given by expression (21). As a result, $I_{cc}(q_z,\vec{q}_\perp)$ is easily shown to become

$$\begin{aligned}I_{cc}(\vec{Q})\propto b^2_{\vec{K}_i}&\int_{-\infty}^{\infty}dz\int_0^\infty \rho\, d\rho J_0(q_\perp\rho)\\&\times\exp\left\{iq_z z-X(K_i)\left[2\gamma+E_1\left(\frac{\rho^2}{4\beta|z|}\right)\right]\right\}\left(\frac{a}{\pi\rho}\right)^{2X(K_i)}\end{aligned} \tag{37}$$

where a first integration over the angular part in the basal xy plane has been performed. The changes of variables $w=\rho^2/4\beta|z|$ and $z'=q_z z$ yield

$$\begin{aligned}I_{cc}(\vec{Q})\propto\sum_i\, b^2_{\vec{K}_i}\frac{1}{q_z^{2-X(K_i)}}&\int_0^\infty dz'\, z'^{1-X(K_i)}\\&\times\exp(iz')\times\int_0^\infty dw\, w^{-X(K_i)}\\&\times\exp[-X(K_i)E_1(w)]J_0\left(2q_\perp\sqrt{\frac{\beta z' w}{q_z}}\right).\end{aligned} \tag{38}$$

Using scaling techniques, the two integrals in Eq. (38) can easily be shown to be proportional to $(q_z/q_\perp^2)^{2-X(K_i)}$, thus yielding

$$I_{cc}(\vec{Q})\propto\sum_i\, b^2_{\vec{K}_i}\frac{1}{q_\perp^{4-2X(K_i)}}\quad\text{for}\ \ q_z=0. \tag{39}$$

The calculation of $I_{cc}(\vec{Q})$ when $q_\perp\simeq 0$ and $q_z\gg q_\perp$ is not explicitly given. The scattering intensity is typical of a crystalline structure [4]. Indeed, under this condition, the system exhibits long-range order behavior, as discussed in the third section of the Appendix. The result is

$$I_{cc}(\vec{Q})\sim\frac{1}{q_z^2}\quad\text{for}\ \ q_\perp=0. \tag{40}$$

C. Thermal diffuse scattering near the Bragg condition due to the periodic orientation density

The thermal diffuse scattering of x rays under these conditions is calculated from $I_{gg}(\vec{Q})$, with a momentum transfer $\vec{Q}=\vec{K}_{hk}+\vec{q}_\perp+3\omega\hat{z}+q_z\hat{z}$, where $\vec{q}_\perp$ and q_z are very small on the scale of the inverse of their respective intermolecular dimension.

It is found that the thermal fluctuations of φ and u_z turn the Bragg peaks at $Q_z=\pm 3\omega$ into Bragg maxima with a universal behavior of the power law decrease of the scattered intensity in reciprocal space. Effectively, near these Bragg conditions, the scattered intensity is written as

$$\begin{aligned}I_{gg}(q_z,\vec{q}_\perp)\propto\int d^3r e^{iq_z z}e^{i\vec{q}_\perp\cdot\vec{\rho}}&\int d^3r'\, e^{-i\vec{Q}\cdot\vec{r}'}\\&\times[e^{i\vec{K}_{hk}\cdot\vec{\rho}}e^{i3\omega z}\langle\rho_g(\vec{r})\rho_g(\vec{r}')\rangle].\end{aligned} \tag{41}$$

where $\vec{r}'=\vec{\rho}_{j'}+\vec{\sigma}'$ (i.e., $\vec{\rho}_{n'm'}=\vec{0}$ and $z'=0$).

As discussed in Sec V B, for $q_z\simeq 0$ and $q_\perp\gg q_z$, the integral (41) is dominated by a cone surrounding the z axis and extending to infinity. The correlation functions of the fluctuating quantities are then given by Eqs. (21) and (23). As shown in Sec. 5 of the Appendix, $I_{gg}(q_z,\vec{q}_\perp)$ becomes

$$\begin{aligned}I_{gg}(\vec{Q})\propto\frac{J_3^2(K_{hk}R_0)}{q_z^{2-X_0'}}&\int_0^\infty dz'\,\exp[iz']z'^{1-X_0'}\int_0^\infty dw\, w^{-X_0'}\exp[-X_0'E_1(w)]\\&\times J_0\left(2q_\perp\sqrt{\frac{w\beta z'}{3q_z}}\right)\prod_{i=1}^4\,\exp[-\xi_i(\tau_i z'^2+\tau'\omega|z'|)^{-1/2}]\\&+\frac{2J_3^2(K_{hk}R_0)\{1+\cos[\vec{q}_\perp\cdot(\vec{\rho}_2-\vec{\rho}_1)]\}}{q_z^{2-X_1'}}\int_0^\infty dz'\,\exp[iz']z'^{1-X_1'}\int_0^\infty dw\, w^{-X_1'}\exp[-X_1'E_1(w)]\\&\times J_0\left(2q_\perp\sqrt{\frac{w\beta z'}{3q_z}}\right)\prod_{i=1}^4\,\exp[-\xi_i(\tau_i z'^2+\tau'\omega|z'|)^{-1/2}],\end{aligned} \tag{42}$$

where $\tau_i = \kappa_i / 9 q_z^2$ and $\tau' = 4\beta / 3|q_z|$. Using scaling techniques, the two integrals in the first term of Eq. (42) are found to be proportional to $q_z^{2-X_0'}/\sqrt{q_\perp}$, while the two integrals in the second term of Eq. (42) are found to be proportional to $q_z^{2-X_1'}/\sqrt{q_\perp}$, leading to

$$I_{gg}(\vec{Q}) \propto \frac{J_3^2(K_{hk}R_0)}{\sqrt{q_\perp}} \{3 + 2\cos[\vec{q}_\perp \cdot (\vec{\rho}_2 - \vec{\rho}_1)]\} \quad \text{for} \quad q_z = 0. \tag{43}$$

As for I_{cc}, the calculation of $I_{gg}(\vec{Q})$ when $q_\perp \simeq 0$ with $q_z \gg q_\perp$ is not explicitly given. The scattering intensity is typical of a crystalline structure [4]. The result is

$$I_{gg}(\vec{Q}) \sim \frac{1}{q_z^2} \quad \text{for} \quad q_\perp = 0. \tag{44}$$

VI. DISCUSSION AND CONCLUSION

It is important to recall that our calculations are based on a model admitting the orderings of the positional and orientational degrees of freedom of the diskotic molecules along the columns, as is generally admitted [5,6,11]. In particular, it is based on the existence of an incommensurate helically ordered density wave along the columnar direction. This density wave results from the ordering of the orientational degrees of freedom. Our model differs from those in the literature only in the range of the ordering, quasi-long-range being speculated in our case.

The separation of the total density $\rho(\vec{r})$ into a core density term $\rho_c(\vec{r})$ and a groove density term $\rho_g(\vec{r})$ is not derived from first principles. In addition, it is clear also that these two quantities are coupled since a core density fluctuation along the columns would break the periodic orientational modulation locally. However, these two quantities refer to independent degrees of freedom to first order: the displacements of the centers of mass of the molecules in the columnar direction and the orientation of the molecules in a plane perpendicular to this direction. This separation captures the two essential features of the density, exactly those features that separately, to lowest order, determine the Bragg conditions for the inverse lattice vectors and the periodic orientational density. Our work is not intended to calculate the intensities of the Bragg maxima but to predict the power law behavior followed by the thermal diffuse x-ray scattering intensities near the Bragg conditions. For such a calculation, we argue that the above separation is justified.

The origin of all the results presented above is the behavior of the denominator of Eq. (13a) governing the rms fluctuations $\langle |u_z(\vec{q})|^2 \rangle_T$. The quadratic form in Eq. (14) reflects the fact that a fluctuation $u_z(\vec{q})$ with a wavelength in the plane perpendicular to the columns very large compared to the length scale of the modulation along the columns, in other words, neighboring columns moving in phase in the columnar direction, is unaffected by the free sliding of the rotating neighboring columns. However, the free sliding of the rotating columns on each other is reflected in the $q_\perp^4$ behavior for a fluctuation $u_z(\vec{q})$ with a wavelength in the plane perpendicular to the columns very small compared to the length scale of the modulation along the columns. It is this last property that gives rise to the quasi-long-range behavior. Indeed, $\langle u_z^2(\vec{r}) \rangle$ shows a quasi-long-range behavior as reflected in Eq. (17). On the contrary, $\langle u_{q_\perp}^2(\vec{r}) \rangle$ shows a long-range behavior as reported in Eq. (19). This last behavior justifies the neglect of $\langle u_{q_\perp}^2 \rangle_T$ in the calculation of the long-tail behavior of the scattered intensities.

The negative sign of the local fluctuation function $\langle u_z(\vec{r}) \varphi(\vec{r}) \rangle$ points to the fact that the independent fluctuating quantity $\Psi(\vec{q})$ is the sum of a rotation $\varphi(\vec{q})$ and a displacement $u_z(\vec{q})$ in the columnar direction, operating in opposite directions in the long-wavelength limit for $q_z \ll q_\perp$, in other words, when neighboring columns are moving more or less rigidly in the columnar direction. Notice that the composite rotation angle $\Psi(\vec{r})$ shows a long-range behavior percolating through the quasi-long-range behaviors of $u_z(\vec{r})$ and $\varphi(\vec{r})$.

The fluctuation correlation functions show a very anisotropic behavior. Indeed, these quantities in the columnar direction have only a quasi-long-range behavior while in the direction perpendicular to the columnar direction a long-range ordering behavior is predicted. As indicated above, these reflect the wave-number dependence of $\langle u_z^2(\vec{r}) \rangle$. As a result, the core density–core density correlation function in the columnar direction shows power law behavior with a series of exponents determined by the elastic constants. The groove density–groove density correlation function in the columnar direction shows a similar power law behavior with exponents related to the helicities of the columns. The correlation functions in the basal plane show long-range behavior.

As mentioned above, our simplified model is not suitable for calculating the relative intensities of the different Bragg peaks. However, it is reasonably justified to calculate the effect of thermal fluctuations on the shape of the Bragg maxima. The first result of interest is that the Bragg peaks in the basal plane $K_{iz} = 0$ retain a behavior typical of long-range ordering. We have not explicitly calculated the effect of the thermal diffuse x-ray scattering and the shape of the intensity contours in this case. This calculation is straightforward and would involve taking in account the effects of the fluctuations $u_{q_\perp}(\vec{q})$. The results would be classical and should show anisotropic intensity contours resulting from the anisotropy of the elastic constants. Such behavior has been studied [14] for freely suspended strands of a diskotic liquid crystal in the intracolumnar disordered phase. It is to be noted that in this last case the Bragg peaks are limited to the $K_{iz} = 0$ plane. Similar behavior has been predicted and observed [15] for the x-ray diffuse scattering in flow-aligned samples of a lyotropic liquid-crystalline hexagonal phase.

The Bragg peaks in the two planes $K_{iz} = \pm C_1$ are turned into Bragg maxima by the thermal fluctuations of the displacement u_z in the columnar direction. In the calculations of the thermal diffuse x-ray scattering intensities, we have omitted the effect of the thermal fluctuations of the displacements in the plane perpendicular to the columns, $u_{q_\perp}(\vec{q})$. This is justified since this last quantity has long-range behavior and would give a contribution only close to the Bragg peaks and not contribute to the long-tail behavior of the scattered intensities. Along the same lines, we have not considered the diffuse scattering from the internal degrees of freedom of the diskotic molecules, i.e., the aliphatic chains for HHTT. We have assumed that such diffuse scattering would not hide the intensity contours predicted here since these degrees of freedom are severely reduced in the ordered columnar phase [5,6]. With the above restrictions, the scattering intensities near the Bragg maxima are shown to have a very anisotropic behavior in reciprocal space, with a nonuniversal behavior typical of quasi-long range ordering in the direction of the columns and a long-range behavior in the basal plane.

Near the Bragg condition for the periodic orientational density, the intensity of the x-ray scattering is predicted to have a very anisotropic power law. In the basal plane, the intensity would decrease with a universal power law $q_\perp^{-1/2}$ for $q_z=0$. The intensity is modulated by the Bessel function of order 3 as expected for an orientationally ordered state in the columnar direction [16]. This last result washes out the Bragg maxima for $K_{hk}=0$. In the columnar direction, this decrease would show q_z^{-2} for $q_\perp=0$.

These behaviors near the Bragg maxima lead us to suggest that high-intensity and high-resolution x-ray scattering measurements should be conducted in order to verify the quasi-long-range behavior in orientationally ordered columnar liquid crystals.

ACKNOWLEDGMENTS

We thank M. L. Plumer for early discussions on the simplified model used in this publication. A.L. would like to thank G. Lamoureux for many helpful references. This work was supported by the Natural Sciences and Engineering Research Council of Canada.

APPENDIX: CALCULATION DETAILS

1. Local correlation functions

As explained in Sec. III, aside from terms whose magnitudes scale with a molecular dimension, the local rms value of the fluctuating variable $u_z(\vec{r})$ is given by

$$\langle u_z^2(\vec{r})\rangle=\frac{k_BT}{4\pi\sqrt{KC_1}}\ln\left(\frac{L_\perp}{a}\right), \tag{A1}$$

an expression increasing with the average size $L_\perp$ of the system in a direction perpendicular to the columns with otherwise infinite length.

From Eqs. (11) and (12) and using the fact that $\Psi(\vec{q})$, $u_z(\vec{q})$, and $u'_{q_\perp}(\vec{q})$ are independent fluctuating quantities, $\langle u_z(\vec{r})\varphi(\vec{r})\rangle$ is written as

$$\langle u_z(\vec{r})\varphi(\vec{r})\rangle=\int\frac{d^3q}{(2\pi)^3}\left(\frac{a\gamma}{4fg_2}-\frac{b}{2f}\right)\langle|u_z(\vec{q})|^2\rangle_T. \tag{A2}$$

The expression in parentheses appearing in the numerator of the integrand of Eq. (A2) has the following long-wavelength power expansion:

$$\frac{a\gamma}{4fg_2}-\frac{b}{2f}=\frac{q_\perp^2(Aq_z^2-Bq_\perp^2)}{Cq_z^4+Dq_z^2+E}, \tag{A3}$$

where A and B are constants and C,D, and E are polynomials with only even powers of $q_\perp$. Looking for the size dependent term, the power expansion (15) is used for $\langle|u_z(\vec{q})|^2\rangle$, the factor (A3) appearing in the numerator being negative under these conditions, $q_z \ll q_\perp$. As a result, we find that the integrand in Eq. (A3) has six simple poles in the complex q_z plane. The three poles located in the upper half plane are at

$$q_z=\frac{i}{\sqrt{2C}}(D\pm\sqrt{D^2-4CE})^{1/2} \tag{A4a}$$

and

$$q_z=i\sqrt{\frac{Kq_\perp^4}{C_1}}. \tag{A4b}$$

The first two poles, in the long-wavelength limit, are at

$$q_z=i\alpha_\pm q_\perp, \tag{A5}$$

where $\alpha_\pm=(D_0\pm\sqrt{D_0^2-4CE_0})^{1/2}/\sqrt{2C}$ with D_0 and E_0 being two constants depending only on the constants of elasticity A_i,B_i,C_i, and K_i. It is found that only the residue at $q_z=i\sqrt{Kq_\perp^4/C_1}$ contributes a term depending on the size of the system. The full integration in the complex space then gives

$$\langle u_z(\vec{r})\varphi(\vec{r})\rangle=-\frac{k_BT}{4\pi\sqrt{KC_1}}\frac{B}{C\alpha_+^2\alpha_-^2}\ln\left(\frac{L_\perp}{a}\right) \tag{A6}$$

and, since $B/C\alpha_+^2\alpha_-^2=B_2/4A_1$, we finally obtain

$$\langle u_z(\vec{r})\varphi(\vec{r})\rangle=-\frac{k_BT}{4\pi\sqrt{KC_1}}\frac{B_2}{4A_1}\ln\left(\frac{L_\perp}{a}\right). \tag{A7}$$

It has been assumed in the previous calculation that the coefficient of $q_\perp^2$ in

$$\begin{aligned}D={}&8C_5(K_1+K_2)q_\perp^4+\{[16A_2(C_2+C_3)+8C_5A_1]\\&-(2B_1+B_2)^2\}q_\perp^2\end{aligned} \tag{A8}$$

is positive. It can be easily shown that a negative value for this coefficient would lead to a divergence of the integral in Eq. (A2) and therefore to an instability, a possibility that we have rejected from the beginning in the formulation of the model.

Finally, the third local fluctuation correlation function to evaluate is

$$\langle \varphi^2(\vec{r})\rangle = \int \frac{d^3q}{(2\pi)^3}\left[\langle|\Psi(\vec{q})|^2\rangle_T + \left(\frac{a\gamma}{4fg_2}-\frac{b}{2f}\right)^2\langle|u_z(\vec{q})|^2\rangle_T + \frac{a^2}{4f^2}\langle|u'_{q_\perp}(\vec{q})|^2\rangle_T\right]. \tag{A9}$$

Each term in the integrand of Eq. (A9) is treated separately. The integration of the first term is straightforward and gives

$$\int \frac{d^3q}{(2\pi)^3}\langle|\Psi(\vec{q})|^2\rangle_T = \frac{k_BT}{4\pi\sqrt{(K_1+K_2)A_2}}\ln(K'+\sqrt{K'^2+1}) \tag{A10}$$

where $K'=(2\pi/a)\sqrt{(K_1+K_2)/A_1}$. An interesting feature of this result is that it is independent of the size of the system, a result typical of long-range ordering. The second term in the integrand of Eq. (A9) is evaluated by following a procedure similar to the one used for Eq. (A2), except that the poles (A4a) are now double poles. The result is found to be

$$\int \frac{d^3q}{(2\pi)^3}\left(\frac{a\gamma}{4fg_2}-\frac{b}{2f}\right)^2\langle|u_z(\vec{q})|^2\rangle_T = \frac{k_BT}{4\pi\sqrt{KC_1}}\frac{B_2^2}{16A_1^2}\ln\left(\frac{L_\perp}{a}\right). \tag{A11}$$

As for Eq. (A2), we have assumed here that the elasticity constants are such that no singularity will appear in the integrand. Finally, the third term in Eq. (A9) is also treated with the help of the residue theorem. Writing

$$\int \frac{d^3q}{(2\pi)^3}\frac{a^2}{4f^2}\langle|u'_{q_\perp}(\vec{q})|^2\rangle_T = k_BT\int\frac{d^3q}{(2\pi)^3}\frac{a^2}{f(4fg_2)} \tag{A12}$$

with the help of Eq. (15), we see upon comparison with Eq. (A2) that the locations of the first two poles in the upper half plane are the same as those given in Eq. (A5). The location of the third one, however, is given by the condition $f=0$, or

$$q_z = iq_\perp\sqrt{\frac{A_1+(K_1+K_2)q_\perp^2}{A_2}} \simeq iq_\perp\sqrt{\frac{A_1}{A_2}} \tag{A13}$$

for small values of $q_\perp$. The three residues contribute equally to the integral over $q_\perp$, leading to

$$\int \frac{d^3q}{(2\pi)^3}\frac{a^2}{4f^2}\langle|u'_{q_\perp}(\vec{q})|^2\rangle_T = \frac{k_BT}{a}\frac{(B_1+B_2)^2}{A_2^2C_5}C', \tag{A14}$$

where

$$C' = \frac{\alpha_+}{(\alpha_+^2+\alpha_-^2)(\alpha_+^2-A_1/A_2)} + \frac{\alpha_-}{(\alpha_-^2+\alpha_+^2)(\alpha_-^2-A_1/A_2)} + \frac{\sqrt{A_1/A_2}}{(A_1/A_2+\alpha_-^2)(A_1/A_2-\alpha_+^2)}. \tag{A15}$$

Again, as in the case of the first term [see Eq. (A10)], the result does not depend on the size of the sample. Finally, putting together Eqs. (A10), (A11), and (A14), we get

$$\langle\varphi^2(\vec{r})\rangle = \frac{k_BT}{4\pi\sqrt{(K_1+K_2)A_2}}\ln(K'+\sqrt{K'^2+1}) + \frac{k_BT}{4\pi\sqrt{KC_1}}\frac{B_2^2}{16A_1^2}\ln\left(\frac{L_\perp}{a}\right) + C'\frac{k_BT}{a}\frac{(B_1+B_2)^2}{A_2^2C_5} \tag{A16}$$

as presented in Eq. (19).

2. Correlation functions along the columns

The correlation function $\langle u_z(\vec{r})u_z(\vec{r}\,')\rangle$ at large distances along the columns (i.e., $|z-z'|\gg c$ and $|\rho-\rho'|$ of the order of a), after an integration of the angular part in the $q_\perp$ plane, is given by

$$\langle u_z(\vec{r})u_z(\vec{r}\,')\rangle = \frac{k_BT}{(2\pi)^2C_1}\int_{2\pi/L_\perp}^{2\pi/a}dq_\perp q_\perp J_0(q_\perp(\rho-\rho')) \times\int_{-\infty}^{\infty}dq_z\frac{e^{-iq_z(z-z')}}{q_z^2+\beta^2q_\perp^4}, \tag{A17}$$

where J_0 is the Bessel function of order 0 and $\beta=\sqrt{K/C_1}$ ($\vec{\rho}$ and $\vec{\rho}\,'$ have both been taken parallel to $\hat{q}_x$ for convenience). The integral over q_z can be performed using the residue theorem, keeping only the simple pole located at $q_z=i\beta q_\perp^2$, leading to

$$\langle u_z(\vec{r})u_z(\vec{r}\,')\rangle = \frac{k_BT}{4\pi\alpha C_1}\int_{2\pi/L_\perp}^{2\pi/a}dq_\perp \times\frac{J_0(q_\perp(\rho-\rho'))}{q_\perp}e^{-\beta q_\perp^2|z-z'|}. \tag{A18}$$

This integral is easily performed to give

$$\langle u_z(\vec{r})u_z(\vec{r}\,')\rangle = \frac{-k_BT}{8\pi\sqrt{KC_1}}\left[2\gamma+E_1\left(\frac{(\rho-\rho')^2}{4\beta|z-z'|}\right)+\ln\left(\frac{\pi^2(\rho-\rho')^2}{L_\perp^2}\right)\right], \tag{A19}$$

where γ is the Euler constant ($\gamma=0.577\,21\ldots$) and $E_1(x)$ is the exponential integral function $E_1(x)=\int_x^\infty(e^{-t}/t)dt$.

The second expression of interest to evaluate is $\langle u_z(\vec{r})\varphi(\vec{r}\,')\rangle$. Using again the same technique applied in Eq. (A2), we have

$$\langle u_z(\vec{r})\varphi(\vec{r}\,')\rangle = \int \frac{d^3q}{(2\pi)^3}\left(\frac{a\gamma}{4fg_2}-\frac{b}{2f}\right) \times\langle|u_z(\vec{q})|^2\rangle_T e^{-i\vec{q}\cdot(\vec{r}-\vec{r}\,')}. \qquad \text{(A20)}$$

The procedure used to evaluate the integral (A20) is almost the same as the one used for $\langle u_z(\vec{r})u_z(\vec{r}\,')\rangle$, except that we now have three poles when integrating over q_z: $q_z=-i(D\pm\sqrt{D^2-4CE})^{1/2}/\sqrt{2C}$, and $q_z=-i\sqrt{Kq_\perp^4/C_1}$. As in the calculation of $\langle u_z(\vec{r})\varphi(\vec{r})\rangle$, the only significant contribution to the integral comes from the residue at $q_z=-i\sqrt{Kq_\perp^4/C_1}$, and we have to evaluate

$$\langle u_z(\vec{r})\varphi(\vec{r}\,')\rangle = -\frac{k_BT}{4\pi\alpha C_1}\frac{B}{C\alpha_+^2\alpha_-^2}\int_{2\pi/L_\perp}^{2\pi/a} dq_\perp \times\frac{J_0(q_\perp(\rho-\rho'))}{q_\perp}e^{-\beta q_\perp^2|z-z'|}, \qquad \text{(A21)}$$

an integral that is identical to the one in Eq. (A18). The final result is then

$$\langle u_z(\vec{r})\varphi(\vec{r}\,')\rangle = \frac{k_BT}{8\pi\sqrt{KC_1}}\frac{B_2}{4A_1}\left[2\gamma+E_1\left(\frac{(\rho-\rho')^2}{4\beta|z-z'|}\right)+\ln\left(\frac{\pi^2(\rho-\rho')^2}{L_\perp^2}\right)\right]. \qquad \text{(A22)}$$

The last expression to evaluate is $\langle\varphi(\vec{r})\varphi(\vec{r}\,')\rangle$ which is written as

$$\langle\varphi(\vec{r})\varphi(\vec{r}\,')\rangle = I_1+I_2+I_3, \qquad \text{(A23)}$$

where

$$I_1=\int\frac{d^3q}{(2\pi)^3}\langle|\Psi(\vec{q})|^2\rangle_T e^{-i\vec{q}\cdot(\vec{r}-\vec{r}\,')}, \qquad \text{(A24a)}$$

$$I_2=\int\frac{d^3q}{(2\pi)^3}\left(\frac{a\gamma}{4fg_2}-\frac{b}{2f}\right)^2\langle|u_z(\vec{q})|^2\rangle_T e^{-i\vec{q}\cdot(\vec{r}-\vec{r}\,')}, \qquad \text{(A24b)}$$

and

$$I_3=\int\frac{d^3q}{(2\pi)^3}\frac{a^2}{4f^2}\langle|u'_{q_\perp}(\vec{q})|^2\rangle_T e^{-i\vec{q}\cdot(\vec{r}-\vec{r}\,')}. \qquad \text{(A24c)}$$

After a first integration of the angular part in the $q_\perp$ plane, I_1 becomes

$$I_1=\frac{k_BT}{(2\pi)^2A_2}\int_{2\pi/L_\perp}^{2\pi/a}dq_\perp q_\perp J_0(q_\perp(\rho-\rho')) \times\int_{-\infty}^{\infty}dq_z\frac{e^{-iq_z(z-z')}}{q_z^2+\eta_1q_\perp^2+\eta_2q_\perp^4}, \qquad \text{(A25)}$$

where $\eta_1=A_1/A_2$ and $\eta_2=(K_1+K_2)/A_2$. Keeping only the simple pole at $q_z=-i\sqrt{\eta_1}q_\perp$ (since again the integrand is dominated by small values of $q_\perp$), we obtain

$$I_1=\frac{k_BT}{4\pi A_2\sqrt{\eta_1}}\int_{2\pi/L_\perp}^{2\pi/a}dq_\perp q_\perp J_0(q_\perp(\rho-\rho'))e^{-\sqrt{\eta_1}q_\perp|z-z'|}. \qquad \text{(A26)}$$

After performing a change of variable $y=\sqrt{\eta_1}|z-z'|q_\perp$, using the power series $J_0(x)=\Sigma_{k=0}^{\infty}(-1)^k(x/2)^{2k}/k!\Gamma(k+1)$ and the function $\Gamma(n)=(n-1)!=\int_0^\infty t^{n-1}e^{-t}dt$ (for $n>0$), we have

$$I_1=\frac{k_BT}{4\pi A_2\sqrt{\eta_1}}\frac{1}{|z-z'|\sqrt{\eta_1}}\sum_{k=0}^{\infty}\frac{(2k)!}{(k!)^2}\left(\frac{-(\rho-\rho')^2}{4\eta_1(z-z')^2}\right)^k. \qquad \text{(A27)}$$

Finally, since $\Sigma_{k=0}^{\infty}(-x)^k(2k)!/(k!)^2=1/\sqrt{1+4x}$, we obtain

$$I_1=\frac{k_BT}{8\pi}\frac{\xi_1}{\sqrt{\kappa_1(z-z')^2+(\rho-\rho')^2}} \qquad \text{(A28)}$$

with $\xi_1=2/\sqrt{A_1A_2}$ and $\kappa_1=\eta_1=A_1/A_2$.

The calculation of I_2 is similar to the one for $\langle u_z(\vec{r})\varphi(\vec{r}\,')\rangle$. Since the integrand now has two double poles at $q_z=-i(D\pm\sqrt{D^2-4CE})^{1/2}/\sqrt{2C}$, the only significant contribution originates from the residue at $q_z=-i\sqrt{Kq_\perp^4/C_1}$. Thus we easily find, upon comparison with Eq. (A20), that

$$I_2=-\frac{k_BT}{8\pi\sqrt{KC_1}}\left(\frac{B_2}{4A_1}\right)^2\left[2\gamma+E_1\left(\frac{(\rho-\rho')^2}{4\beta|z-z'|}\right)+\ln\left(\frac{\pi^2(\rho-\rho')^2}{L_\perp^2}\right)\right]. \qquad \text{(A29)}$$

Finally, after an integration over the angular contribution in the $q_\perp$ plane, I_3 yields

$$I_3=\frac{k_BT}{(2\pi)^2}\frac{\left(B1+\frac{1}{2}B_2\right)^2}{4}\int_{2\pi/L_\perp}^{2\pi/a}dq_\perp q_\perp^3J_0(q_\perp(\rho-\rho')) \times\int_{-\infty}^{\infty}dq_zq_z^2\frac{e^{-iq_z(z-z')}}{(Cq_z^4+Dq_z^2+E)f}, \qquad \text{(A30)}$$

where C, D, and E are the same functions as those defined in Eq. (A3). As found previously in the development of the third term in the integrand of Eq. (A9), the integrand of I_3 has four simple poles at $q_z=\pm i\alpha_{\pm}q_{\perp}$ and the condition $f=0$ yields two more simple poles at $q_z=\pm i\sqrt{A_1/A_2}q_{\perp}$. We finally find, after an integration over $q_{\perp}$,

$$I_3=\frac{k_BT}{8\pi}\sum_{i=2}^{4}\frac{\xi_i}{\sqrt{\kappa_i(z-z')^2+(\rho-\rho')^2}} \tag{A31}$$

with the following definitions:

$$\xi_2=\frac{-\left(B_1+\frac{1}{2}B_2\right)^2\alpha_+}{(\alpha_+^2-\alpha_-^2)(\alpha_+^2-A_1/A_2)}, \tag{A32a}$$

$$\xi_3=\frac{-\left(B_1+\frac{1}{2}B_2\right)^2\alpha_-}{(\alpha_-^2-\alpha_+^2)(\alpha_-^2-A_1/A_2)}, \tag{A32b}$$

and

$$\xi_4=\frac{-\left(B_1+\frac{1}{2}B_2\right)^2\sqrt{A_1/A_2}}{(A_1/A_2-\alpha_-^2)(A_1/A_2-\alpha_+^2)}. \tag{A32c}$$

and $\kappa_2=\alpha_+^2$, $\kappa_3=\alpha_-^2$, and $\kappa_4=A_1/A_2$. It is found numerically that the value of I_3 is positive for $|z-z'|\gg c$ and $|\rho-\rho'|\simeq a$, which is precisely the limit used for the present calculations.

Thus, combining Eqs. (A28), (A29), and (A31), we obtain

$$\begin{aligned}\langle\varphi(\vec{r})\varphi(\vec{r}\,')\rangle={}&\frac{k_BT}{8\pi}\sum_{i=1}^{4}\frac{\xi_i}{\sqrt{\kappa_i(z-z')^2+(\rho-\rho')^2}}\\&-\frac{k_BT}{8\pi\sqrt{KC_1}}\frac{B_2^2}{16A_1^2}\left[2\gamma+E_1\left(\frac{(\rho-\rho')^2}{4\beta|z-z'|}\right)\right.\\&\left.+\ln\left(\frac{\pi^2(\rho-\rho')^2}{L_\perp^2}\right)\right]\end{aligned} \tag{A33}$$

as presented in Eq. (23).

3. Correlation functions in the plane perpendicular to the columnar direction

The correlations at large distances in the plane perpendicular to the columnar direction, i.e., $|z-z'|\ll c$ and $|\rho-\rho'|\gg a$, are easily obtained. Indeed, referring to Eq. (20), they are dominated by small values of $q_\perp$ and an integration over all values of q_z. The limit $q_z\gg q_\perp$ is then justified. From the denominator expression (14), the correlation functions are anticipated to have a behavior typical of long-range ordering. Expressions having a structure similar to Eq. (A28) are then obtained as expected for random fluctuations for long-range ordering.

For example, the value of $\langle u_z(\vec{r})u_z(\vec{r}\,')\rangle$ is explicitly given by

$$\begin{aligned}\langle u_z(\vec{r})u_z(\vec{r}\,')\rangle={}&\frac{k_bT}{C_1(2\pi)^2}\int_{2\pi/L_\perp}^{2\pi/a}q_\perp J_0(q_\perp\rho)dq_\perp\\&\times\int_{-\infty}^{\infty}dq_z\frac{e^{-iq_zz}}{q_z^2+\beta^2q_\perp^2},\end{aligned} \tag{A34}$$

where $\beta=\sqrt{G/C_1}$. The integrations are easily performed and yield

$$\langle u_z(\vec{r})u_z(\vec{r}\,')\rangle=\frac{k_BT}{4\pi\sqrt{KC_1}}\frac{1}{\sqrt{\alpha^2(z-z')^2+(\rho-\rho')^2}}, \tag{A35}$$

an expression having a structure similar to Eq. (A28). The results for $\langle u_z(\vec{r})\varphi(\vec{r}\,')\rangle$ and $\langle\varphi(\vec{r})\varphi(\vec{r}\,')\rangle$ give similar structures.

4. Density-density correlation function in the columnar direction

In this section, we present the calculations performed to evaluate explicitly the function

$$\begin{aligned}G(\vec{r}-\vec{r}\,')={}&\langle\rho_c(\vec{r})\rho_c(\vec{r}\,')\rangle+\langle\rho_c(\vec{r})\rho_g(\vec{r}\,')\rangle+\langle\rho_g(\vec{r})\rho_c(\vec{r}\,')\rangle\\&+\langle\rho_g(\vec{r})\rho_g(\vec{r}\,')\rangle.\end{aligned} \tag{A36}$$

The first term in Eq. (A36) is explicitly given by

$$\begin{aligned}\langle\rho_c(\vec{r})\rho_c(\vec{r}\,')\rangle={}&\sum_i\sum_{i'}b_{\vec{K}_i}b_{\vec{K}_{i'}}\langle\cos\{K_{i\perp}\rho\cos\alpha\\&+K_{iz}[z-u_z(\vec{r})]\}\cos\{K_{i'\perp}\rho'\cos\alpha\\&+K_{i'z}[z'-u_z(\vec{r}\,')]\}\rangle.\end{aligned} \tag{A37}$$

$\vec{\rho}$ and $\vec{\rho}\,'$ have been taken parallel. Using the property $\langle\exp[\alpha_ix_i]\rangle_T=\exp[\alpha_i\alpha_k\langle x_ix_k\rangle_T/2]$, Eq. (A37) becomes

$$\begin{aligned}\langle\rho_c(\vec{r})\rho_c(\vec{r}\,')\rangle={}&\frac{1}{4}\sum_i\sum_{i'}(F_1\exp\{-[(K_{iz}^2+K_{i'z}^2)\langle u_z^2(\vec{r})\rangle\\&+2K_{iz}K_{i'z}\langle u_z(\vec{r})u_z(\vec{r}\,')\rangle]\}\\&+F_2\exp\{-[(K_{iz}^2+K_{i'z}^2)\langle u_z^2(\vec{r})\rangle\\&-2K_{iz}K_{i'z}\langle u_z(\vec{r})u_z(\vec{r}\,')\rangle]\}),\end{aligned} \tag{A38}$$

where $F_1=2b_{\vec{K}_i}b_{\vec{K}_{i'}}\cos(\vec{K}_i\cdot\vec{r}+\vec{K}_{i'}\cdot\vec{r}\,')$ and $F_2=2b_{\vec{K}_i}b_{\vec{K}_{i'}}\cos(\vec{K}_i\cdot\vec{r}-\vec{K}_{i'}\cdot\vec{r}\,')$. After substitution of Eqs. (17) and (A19) in Eq. (A38), we find that $\langle\rho_c(\vec{r})\rho_c(\vec{r}\,')\rangle$ depends only on $|\vec{r}-\vec{r}\,'|$ (and consequently is independent of $L_\perp$) if and only if $\vec{K}_i=-\vec{K}_{i'}$ [for the first term in Eq. (A38)] or $\vec{K}_i=\vec{K}_{i'}$ (for the second term in Eq. (A38)]. This condition is required by the overall translational invariance of the system. Consequently, we find

$$\begin{aligned}\langle \rho_c(\vec{r})\rho_c(\vec{r}\,')\rangle = \frac{1}{2}\sum_{i}\sum_{i'} b_{\vec{K}_i} b_{\vec{K}_{i'}} [\cos(\vec{K}_i\cdot\vec{r}+\vec{K}_{i'}\cdot\vec{r}\,')\\ \times \delta_{\vec{K}_i,-\vec{K}_{i'}} + \cos(\vec{K}_i\cdot\vec{r}-\vec{K}_{i'}\cdot\vec{r}\,')\,\delta_{\vec{K}_i,\vec{K}_{i'}}]\\ \times \exp\left\{-X(K_{iz})\left[2\gamma+E_1\left(\frac{(\rho-\rho')^2}{4\beta|z-z'|}\right)\right]\right\}\\ \times\left(\frac{a}{\pi|\rho-\rho'|}\right)^{2X(K_{iz})},\end{aligned}\tag{A39}$$

or, using the development $E_1(x)\simeq -\gamma-\ln(x)$ for $x\ll 1$,

$$\begin{aligned}\langle \rho_c(\vec{r})\rho_c(\vec{r}\,')\rangle \sim \sum_i b^2_{\vec{K}_i}\cos\vec{K}_i\cdot(\vec{r}-\vec{r}\,')\\ \times\left(\frac{a^2}{4\pi^2\beta|z-z'|}\right)^{X(K_{iz})},\end{aligned}\tag{A40}$$

where $X(K_{iz})=K_{iz}^2(k_BT/8\pi\sqrt{KC_1})$.

The second term in Eq. (24) is given by

$$\begin{aligned}\langle \rho_c(\vec{r})\rho_g(\vec{r}\,')\rangle = \frac{\rho_{g0}}{4}\sum_i\sum_{n',m'}\sum_{j'=0}^{2} b_{\vec{K}_i}\delta(\vec{\rho}\,'-(\vec{\rho}_{n'm'}+\vec{\rho}_{j'}\\ +\vec{\sigma}\,'))\langle\cos\{K_{i\perp}\rho\cos(\alpha_\perp-\alpha_i)\\ +K_{iz}[z-u_z(\vec{r})]\}\\ \times\cos 3\{\theta'-H_{j'}\omega[z'-u_z(\vec{r}\,')]\\ -[\Omega_{j'}-\varphi(\vec{r}\,')]\}\rangle.\end{aligned}\tag{A41}$$

It can be written, with the help of Eq. (25), as

$$\begin{aligned}\langle \rho_c(\vec{r})\rho_g(\vec{r}\,')\rangle = \rho_{g0}\sum_i\sum_{n',m'}\sum_{j'=0}^{2}\left[F_1\exp\left(-\frac{1}{2}U_1\right)\right.\\ \left.+F_2\exp\left(-\frac{1}{2}U_2\right)\right],\end{aligned}\tag{A42}$$

where

$$\begin{aligned}U_1=(K_{iz}^2+9\omega^2)\langle u_z^2(\vec{r})\rangle+9\langle\varphi^2(\vec{r})\rangle\\ -6K_{iz}H_{j'}\omega\langle u_z(\vec{r})u_z(\vec{r}\,')\rangle-6K_{iz}\langle u_z(\vec{r})\varphi(\vec{r}\,')\rangle\\ +18H_{j'}\omega\langle u_z(\vec{r}\,')\varphi(\vec{r}\,')\rangle,\end{aligned}\tag{A43a}$$

$$\begin{aligned}U_2=(K_{iz}^2+9\omega^2)\langle u_z^2(\vec{r})\rangle+9\langle\varphi^2(\vec{r})\rangle\\ +6K_{iz}H_{j'}\omega\langle u_z(\vec{r})u_z(\vec{r}\,')\rangle+6K_{iz}\langle u_z(\vec{r})\varphi(\vec{r}\,')\rangle\\ +18H_{j'}\omega\langle u_z(\vec{r}\,')\varphi(\vec{r}\,')\rangle,\end{aligned}\tag{A43b}$$

$$\begin{aligned}F_1=2b_{\vec{K}_i}\delta(\vec{\rho}\,'-(\vec{\rho}_{n'm'}+\vec{\rho}_{j'}+\vec{\sigma}\,'))\\ \times\cos[\vec{K}_i\cdot\vec{r}-3(-\theta'+H_{j'}\omega z'+\Omega_{j'})],\end{aligned}\tag{A44a}$$

$$\begin{aligned}F_2=2b_{\vec{K}_i}\delta(\vec{\rho}\,'-(\vec{\rho}_{n'm'}+\vec{\rho}_{j'}+\vec{\sigma}\,'))\\ \times\cos[\vec{K}_i\cdot\vec{r}+3(-\theta'+H_{j'}\omega z'+\Omega_{j'})].\end{aligned}\tag{A44b}$$

Substituting Eqs. (17), (A7), (A16), (A19), and (A22) into Eq. (A43), we find that Eq. (A42) depends on $|\vec{r}-\vec{r}\,'|$ if and only if

$$K_{iz}=\pm 3\left(H_j\omega-\frac{B_2}{4A_1}\right).\tag{A45}$$

Rewriting Eq. (A16) as

$$\langle\varphi^2(\vec{r})\rangle=F_0+\frac{k_BT}{4\pi\sqrt{KC_1}}\frac{B_2^2}{16A_1^2}\ln\left(\frac{L_\perp}{a}\right),\tag{A46}$$

where

$$\begin{aligned}F_0=\frac{k_BT}{4\pi\sqrt{(K_1+K_2)A_2}}\ln(K'+\sqrt{K'^2+1})\left(\frac{L_\perp}{a}\right)\\ -C'\frac{k_BT}{a}\frac{(B_1+B_2)^2}{A_2^2C_5},\end{aligned}\tag{A47}$$

we finally find

$$\begin{aligned}\langle \rho_g(\vec{r})\rho_c(\vec{r}\,')\rangle = \frac{\rho_{g0}}{4}\sum_i\sum_{n',m'}\sum_{j'=0}^{2}(F_1+F_2)\\ \times\exp\left\{-X'_{j'}\left[2\gamma+E_1\left(\frac{(\rho-\rho')^2}{4\beta|z-z'|}\right)\right]\right.\\ \left.-\frac{9}{2}F_0\right\}\left(\frac{a}{\pi|\rho-\rho'|}\right)^{X'_{j'}}\\ \times\delta_{K_{iz},\pm 3(H_j\omega-B_2/4A_1)},\end{aligned}\tag{A48}$$

where

$$X'_{j'}=\frac{9k_BT}{8\pi\sqrt{KC_1}}\left[H_j\omega-\left(\frac{B_2}{4A_1}\right)\right]^2.\tag{A49}$$

The third term in Eq. (24), $\langle\rho_g(\vec{r})\rho_c(\vec{r}\,')\rangle$, is obtained exactly like the second one, and the result is identical to Eq. (A48), with the changes $i\to i'$, $n'\to n$, $m'\to m$, and $j'\to j$. Finally, the fourth term in Eq. (24) can be explicitly written as

$$\begin{aligned}\langle\rho_g(\vec r)\rho_g(\vec r\,')\rangle\\ &=\rho_{g0}^2\sum_{n,m}\sum_{n',m'}\sum_{j=0}^{2}\sum_{j'=0}^{2}\delta(\vec\rho-(\vec\rho_{nm}+\vec\rho_j+\vec\sigma))\\ &\quad\times\delta(\vec\rho\,'-(\vec\rho_{n'm'}+\vec\rho_{j'}+\vec\sigma\,'))\\ &\quad\times\langle\cos3\{\theta-H_j\omega[z-u_z(\vec r)]-[\Omega_j-\varphi(\vec r)]\}\\ &\quad\times\cos3\{\theta'-H_{j'}\omega[z'-u_z(\vec r\,')]-[\Omega_{j'}-\varphi(\vec r\,')]\}\rangle.\end{aligned}\tag{A50}$$

Using the property (25), we find

$$\begin{aligned}\langle\rho_g(\vec r)\rho_g(\vec r\,')\rangle=\frac{\rho_{g0}^2}{4}\sum_{n,m}\sum_{n',m'}\sum_{j=0}^{2}\sum_{j'=0}^{2}\Bigg[F_1\exp\left(-\frac{1}{2}U_1\right)\\ +F_2\exp\left(-\frac{1}{2}U_2\right)\Bigg],\end{aligned}\tag{A51}$$

where

$$\begin{aligned}U_1=18\{&\omega^2\langle u_z^2(\vec r)\rangle+\langle\varphi^2(\vec r)\rangle+H_jH_{j'}\omega^2\langle u_z(\vec r)u_z(\vec r\,')\rangle\\ &+H_j\omega[\langle u_z(\vec r)\varphi(\vec r\,')\rangle+\langle u_z(\vec r)\varphi(\vec r)\rangle]\\ &+H_{j'}\omega[\langle\varphi(\vec r)u_z(\vec r\,')\rangle+\langle\varphi(\vec r\,')u_z(\vec r\,')\rangle]\\ &+\langle\varphi(\vec r)\varphi(\vec r\,')\rangle\},\end{aligned}\tag{A52a}$$

$$\begin{aligned}U_2=18\{&\omega^2\langle u_z^2(\vec r)\rangle+\langle\varphi^2(\vec r)\rangle-H_jH_{j'}\omega^2\langle u_z(\vec r)u_z(\vec r\,')\rangle\\ &+H_j\omega[-\langle u_z(\vec r)\varphi(\vec r\,')\rangle+\langle u_z(\vec r)\varphi(\vec r)\rangle]\\ &+H_{j'}\omega[-\langle\varphi(\vec r)u_z(\vec r\,')\rangle+\langle\varphi(\vec r\,')u_z(\vec r\,')\rangle]\\ &-\langle\varphi(\vec r)\varphi(\vec r\,')\rangle\},\end{aligned}\tag{A52b}$$

$$\begin{aligned}F_1=&\,\delta(\vec\rho-(\vec\rho_{nm}+\vec\rho_j+\vec\sigma))\delta(\vec\rho\,'-(\vec\rho_{n'm'}+\vec\rho_{j'}+\vec\sigma\,'))\\ &\times\cos3[\theta-H_j\omega z-\Omega_j+(\theta'-H_{j'}\omega z'-\Omega_{j'})],\end{aligned}\tag{A53a}$$

and

$$\begin{aligned}F_2=&\,\delta(\vec\rho-(\vec\rho_{nm}+\vec\rho_j+\vec\sigma))\delta(\vec\rho\,'-(\vec\rho_{n'm'}+\vec\rho_{j'}+\vec\sigma\,'))\\ &\times\cos3[\theta-H_j\omega z-\Omega_j-(\theta'-H_{j'}\omega z'-\Omega_{j'})].\end{aligned}\tag{A53b}$$

As before, we substitute Eqs. (17), (A7), (A16), (A19), (A22), and (A33) into Eqs. (A52). Then we evaluate, for both cases $H_j=H_{j'}$ and $H_j=-H_{j'}$, the conditions under which U_1 and U_2 will depend on $|\vec r-\vec r\,'|$. It is found that U_1 meets this requirement when $H_j=H_{j'}=1$ and $\omega=B_2/4A_1$, a condition that is too restrictive. However, U_2 meets this requirement provided $H_j=H_{j'}$. Effectively, under this last condition, we have

$$\begin{aligned}U_2=2X_j'\left[2\gamma+E_1\left(\frac{(\rho-\rho')^2}{4\beta|z-z'|}\right)+\ln\left(\frac{\pi^2(\rho-\rho')^2}{a^2}\right)\right]\\ -9F(\vec r-\vec r\,'),\end{aligned}\tag{A54}$$

where

$$F(\vec r-\vec r\,')=\frac{k_BT}{8\pi}\sum_{i=1}^{4}\frac{\xi_i}{\sqrt{\kappa_i(z-z')^2+(\rho-\rho')^2}}+F_0\tag{A55}$$

and X_j' is given by Eq. (A49). The final result for the fourth term of Eq. (24) is

$$\langle\rho_g(\vec r)\rho_g(\vec r\,')\rangle=\frac{\rho_{g0}^2}{4}\sum_{n,m}\sum_{n',m'}\sum_{j=0}^{2}\sum_{j'=0}^{2}F_2\exp\left(-\frac{1}{2}U_2\right),\tag{A56}$$

with the function U_2 given in Eq. (A54) or, using again the development $E_1(x)\simeq-\gamma-\ln(x)$ for $x\ll1$ and the fact that $F(\vec r-\vec r\,')\simeq F_0$ for large distances,

$$\langle\rho_g(\vec r)\rho_g(\vec r\,')\rangle\sim\sum_{j=0}^{2}F_2\left(\frac{a^2}{4\pi^2\beta|z-z'|}\right)^{X_j'}.\tag{A57}$$

5. Scattered intensity calculations

This section presents the calculations pertaining to the thermal diffuse scattering near the Bragg condition due to the periodic orientation density for $q_z\simeq0$ and $q_\perp\gg q_z$. As mentioned in the text, the effect of the thermal diffuse scattering near these Bragg conditions is calculated from $I_{gg}(\vec Q)$, which is evaluated by taking $\vec r\,'=\vec\rho_{j'}+\vec\sigma\,'$ (i.e., $\vec\rho_{n'm'}=\vec 0$ and $z'=0$) for a momentum transfer $\vec Q=\vec K_{hk}+\vec q_\perp+3\omega\hat z+q_z\hat z$, with $\vec q_\perp$ and q_z very small on the scale of the inverse of their respective intermolecular dimensions. For $q_z=0$ and $q_\perp\gg q_z$, the integral $I_{gg}(\vec r)$ is dominated by a cone surrounding the z axis. After a first integration over the basal xy plane, we obtain

$$\begin{aligned}I_{gg}(\vec Q)\propto\sum_{\{j,j'\}}\sum_{nm}\int_{-\infty}^{\infty}dz\int_0^{2\pi}d\theta\int_0^{2\pi}d\theta'(\exp[i3\Phi]\\ +\exp[-i3\Phi])\exp\left\{-X_j'\left[2\gamma+E_1\left(\frac{\rho_{nmj}^2}{4\beta|z|}\right)\right]\right\}\\ \times\left(\frac{a}{\pi\rho_{nmj}}\right)^{2X_j'}\exp\Bigg[-\frac{9}{2}\Bigg(F_0+\sum_{i=1}^{4}\xi_i(\kappa_iz^2\\ +\rho_{nmj}^2)^{-1/2}\Bigg)\Bigg]\exp[i(\vec K_{hk}+\vec q_\perp)(\vec\rho_{nmj}+\vec\sigma-\vec\rho_{j'}\\ -\vec\sigma\,')]\exp[i(3\omega+q_z)z],\end{aligned}\tag{A58}$$

where $\Phi=\theta-\theta'-[\theta_{0j}(z)-\theta_{0j'}(0)]$, $\vec{\rho}_{nmj}=\vec{\rho}_{nm}+\vec{\rho}_j$, and $\{j,j'\}$ represents the pairs of indices (j,j') that are such that $H_j=H_{j'}$. Integration over the angular contribution within the columns and summation over the six given couples (j,j') yields

$$\begin{aligned}I_{gg}(\vec{Q})\propto&\int_0^\infty\rho\;\;d\rho\int_{-\infty}^\infty dz\;\;J_3^2(K_{hk}R_0)\exp[i3q_zz]\exp\left[-\frac{9}{2}\left(F_0+\sum_{i=1}^4\xi_i(\kappa_iz^2+\rho^2)^{-1/2}\right)\right]\\&\times\exp\left\{-X_0'\left[2\gamma+E_1\left(\frac{\rho^2}{4\beta|z|}\right)\right]\right\}\left(\frac{a}{\pi\rho}\right)^{2X_0'}J_0(q_\perp\rho)+\int_0^\infty\rho\,d\rho\int_{-\infty}^\infty dz\;\;J_3^2(K_{hk}R_0)\exp[i3q_zz]\\&\times\exp\left[-\frac{9}{2}\left(F_0+\sum_{i=1}^4\xi_i(\kappa_iz^2+\rho^2)^{-1/2}\right)\right]\\&\times2\,\exp\left\{-X_1'\left[2\gamma+E_1\left(\frac{\rho^2}{4\beta|z|}\right)\right]\right\}\left(\frac{a}{\pi\rho}\right)^{2X_1'}\{1+\cos[\vec{q}_\perp\cdot(\vec{\rho}_2-\vec{\rho}_1)]\}J_0(q_\perp\rho),\end{aligned}\tag{A59}$$

where we have neglected $|\vec{\rho}_j|$ in front of $|\vec{\rho}_{nm}|$ and extended the infinite sum over ρ_{nm} to an integral over the continuous variable ρ. With the changes of variables $w=\rho^2/4\beta|z|$ and $z'=3q_zz$, Eq. (A59) can be rewritten as

$$\begin{aligned}I_{gg}(\vec{G})\propto&\frac{J_3^2(K_{hk}R_0)}{q_z^{2-X_0'}}\int_0^\infty dz'\;\exp[(iz')z'^{1-X_0'}]\int_0^\infty dw\;\;w^{-X_0'}\exp[-X_0'E_1(w)]\\&\times J_0\left(2q_\perp\sqrt{\frac{w\beta z'}{3q_z}}\right)\prod_{i=1}^4\;\exp[-\xi_i(\tau_iz'^2+\tau'\omega|z'|)^{-1/2}]\\&+\frac{2J_3^2(K_{hk}R_0)\{1+\cos[\vec{q}_\perp\cdot(\vec{\rho}_2-\vec{\rho}_1)]\}}{q_z^{2-X_1'}}\int_0^\infty dz'\;\exp[(iz')z'^{1-X_1'}]\int_0^\infty dw\;\;w^{-X_1'}\exp[-X_1'E_1(w)]\\&\times J_0\left(2q_\perp\sqrt{\frac{w\beta z'}{3q_z}}\right)\prod_{i=1}^4\;\exp[-\xi_i(\tau_iz'^2+\tau'\omega|z'|)^{-1/2}],\end{aligned}\tag{A60}$$

where $\tau_i=\kappa_i/9q_z^2$ and $\tau'=4\beta/3|q_z|$, as presented in Eq. (42). Using scaling techniques, the two integrals in the first term of Eq. (A60) are found to be proportional to $q_z^{2-X_0'}/\sqrt{q_\perp}$, while the two integrals in the second term of Eq. (A60) are found to be proportional to $q_z^{2-X_1'}/\sqrt{q_\perp}$, leading to

$$I_{gg}(\vec{Q})\propto\frac{J_3^2(K_{hk}R_0)}{\sqrt{q_\perp}}\{3+2\,\cos[\vec{q}_\perp\cdot(\vec{\rho}_2-\vec{\rho}_1)]\}.\tag{A61}$$

---

[1] A. Caillé, C. R. Seances Acad. Sci., Ser. B **274**, 891 (1972).
[2] J. Als-Nielsen, R.J. Birgeneau, M. Kaplan, J.D. Litster, and C.R. Safinya, Phys. Rev. Lett. **39**, 1668 (1977).
[3] J. Als-Nielsen, J.D. Litster, R.J. Birgeneau, M. Kaplan, C.R. Safinya, A. Lindegaard-Andersen, and S. Mathiesen, Phys. Rev. B **22**, 312 (1980).
[4] P.-G. de Gennes and J. Prost, *The Physics of Liquid Crystals*, 2nd ed. (Oxford University Press, New York, 1993).
[5] E. Fontes, P.A. Heiney, and W.H. de Jeu, Phys. Rev. Lett. **61**, 1202 (1988).
[6] P.A. Heiney, E. Fontes, W.H. de Jeu, A. Riera, P. Carroll, and A.B. Smith III, J. Phys. (France) **50**, 461 (1989).
[7] A.M. Levelut, J. Phys. (France) Lett. **40**, L81 (1979).
[8] S. Chandrasekhar and G.S. Ranganath, Rep. Prog. Phys. **53**, 57 (1990).
[9] H.R. Brand and H. Pleiner, Phys. Rev. Lett. **69**, 987 (1992).
[10] G. Durand, Phys. Rev. Lett. **69**, 988 (1992).
[11] A. Caillé and Matthieu Hébert, Phys. Rev. E **54**, R4544 (1996).
[12] L. Landau and E. Lifshitz, *Statistical Physics, Part 1*, 3rd ed. (Pergamon Press, New York, 1980).
[13] S. Idziak, Ph.D. dissertation, University of Pennsylvania, 1989.
[14] P. Davidson, M. Clerc, S.S. Ghosh, N.C. Maliszewskyj, P.A. Heiney, J. Hynes, Jr., and A.B. Smith III, J. Phys. II **5**, 249 (1995).
[15] M. Impéror-Clerc and P. Davidson, Eur. Phys. J. B **9**, 93 (1999).
[16] J.D. Watson and F.H.C. Crick, Nature (London) **171**, 737 (1953).